DOI: 10.1002/ejoc.200800547

Biomimetic Self-Assembly of Tetrapeptides into Fibrillar Networks and Organogels

Sajid Iqbal,[a] Juan F. Miravet,*[a] and Beatriu Escuder*[a]

Keywords: Self-assembly / Gels / Peptides / Silk / Fibers / Protein folding

The self-assembly features of a family of tetrapeptides with a silk-inspired structure are presented. An exhaustive study of the influence of the terminal alkyl chain length in this process is undertaken. Scanning electron microscopy (SEM), wide-angle X-ray diffraction (WAXD), FTIR spectroscopy, and circular dichroism were used for structural analysis. These compounds, as in the natural model, self-assemble into antiparallel β-sheet structures that further organize to form fibrillar aggregates. Furthermore, some of them are capable of forming a crowded network that entraps the solvent leading to physical gels with different microscopic morphologies. A model for the assembly process is proposed.

Introduction

Nature's high complexity and efficiency has always attracted the attention of scientists, firstly to unravel its fascinating structures and processes and subsequently intending to imitate the beauty and harmony of them. For instance, mimicking the natural control of the conformation of biomolecules at the different levels of complexity and function has been an appealing goal. In this sense, the study of protein structure and function has created a wide interest.[1,2] It is well known that the different organization levels play an important role in different structural and functional proteins. For example, structural proteins (i.e. collagen, elastin, and silks) base their physical properties in different aspects of their secondary structure. On the other hand, precisely folded switch points determine the active sites in catalytic proteins and enzymes.[3] Furthermore, some devastating diseases such as amyloidogenic pathologies are related to anomalous protein folding that induces precipitation of toxic plaques. Recently, intense research has been devoted to the understanding of the amyloid aggregation mechanisms as well as to the development of strategies to prevent this unwanted process.[4]

In this context, the study of model systems, including peptides and small peptidomimetics, that self-assemble into fibrillar aggregates may help to determine the molecular basis for such processes.[5–8] In connection with these studies, the formation of self-assembled fibrillar networks and gels from low molecular weight molecules has been studied extensively in the recent past. Many efforts in this field are directed towards an understanding of the role that the different structural elements present in the gelators play in the noncovalent association that yields the final fibrillar structures.[9–11]

In the last years we have been involved in the study of low-molecular weight gelators based on amino acids. These small peptidomimetic compounds self-assemble into sheet-like extended structures that form fibrous aggregates and gels in different solvents.[12] Recently, we have reported the design of a novel tetrapeptidic organogelator (**4**) based on a minimal sequence found in silks, Gly–L-Ala–Gly–L-Ala, and incorporating C_{12} alkyl chains at both ends of the tetrapeptide.[13] We studied its self-assembly in organic solvents and it was revealed that this sequence showed a high preference for the antiparallel assembly into β-sheets (Scheme 1).

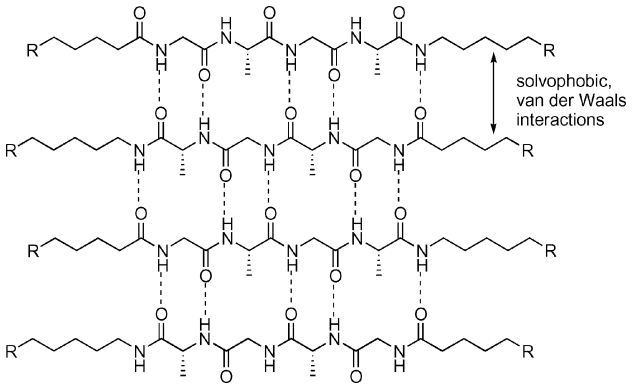

Scheme 1.

[a] Departament de Química Inorgànica i Orgànica, Universitat Jaume I,
12071 Castelló, Spain
Fax: +34-964729155
E-mail: escuder@qio.uji.es

Supporting information for this article is available on the WWW under http://www.eurjoc.org or from the author.

In natural silk proteins, specific amino acids induce a turn in the polypeptidic chain causing its preorganization for an antiparallel β-sheet. In contrast, it is remarkable that in the reported gelator the "folding effect" was driven only by noncovalent interactions. We believe that this naturally selected one-dimensional assembly motif has a great potential for the design of new functional fibrous nanomaterials.

Here we report on the preparation and study of a library of compounds based on the variation of the terminal groups attached to the silk-mimetic tetrapeptide motif Gly–L-Ala–Gly–L-Ala (Scheme 2). Our aims include to clarify how the interplay of the noncovalent interactions provided by the apolar end moieties and the peptide core affect the self-assembly of these molecules. The different nature of the intermolecular interactions provided by these moieties (van der Waals and solvophobic/solvophylic in one case and hydrogen bonding in the other case) is expected to allow fine tuning of the aggregation behavior with the use of, for example, of a variety of solvents. We are interested in assessing how properties such size and aspect of the microscopic fibers, gelation of different solvents, antiparallel peptide arrangement, or microcrystalline packing are changed through a family of structurally related molecules.

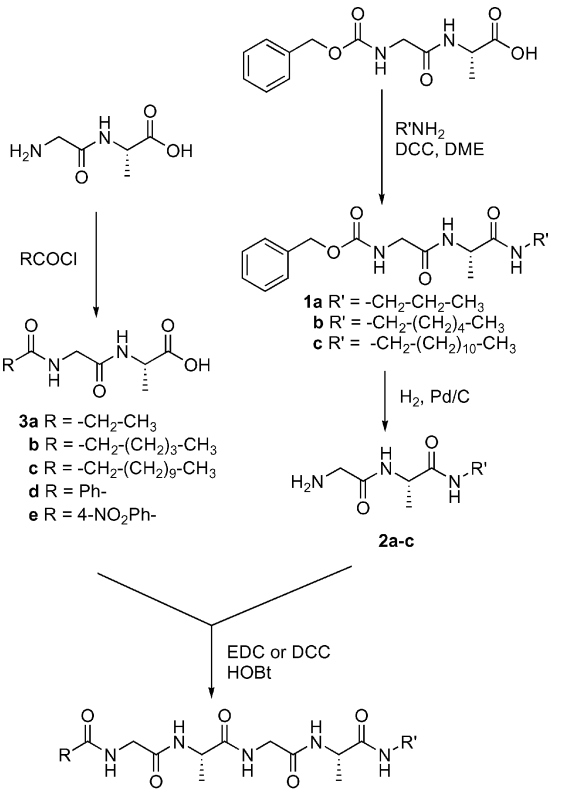

4	R = $-CH_2-(CH_2)_9-CH_3$	R' = $-CH_2-(CH_2)_{10}-CH_3$
5	R = $-CH_2-(CH_2)_3-CH_3$	R' = $-CH_2-(CH_2)_4-CH_3$
6	R = $-CH_2-CH_3$	R' = $-CH_2-CH_2-CH_3$
7	R = $-CH_2-(CH_2)_9-CH_3$	R' = $-CH_2-(CH_2)_4-CH_3$
8	R = $-CH_2-(CH_2)_9-CH_3$	R' = $-CH_2-CH_2-CH_3$
9	R = $-CH_2-(CH_2)_3-CH_3$	R' = $-CH_2-(CH_2)_{10}-CH_3$
10	R = $-CH_2-(CH_2)_3-CH_3$	R' = $-CH_2-CH_2-CH_3$
11	R = $-CH_2-CH_3$	R' = $-CH_2-(CH_2)_{10}-CH_3$
12	R = $-CH_2-CH_3$	R' = $-CH_2-(CH_2)_4-CH_3$
13	R = Ph-	R' = $-CH_2-CH_2-CH_3$
14	R = 4-NO_2Ph-	R' = $-CH_2-CH_2-CH_3$
15	R = Ph-	R' = $-CH_2-(CH_2)_4-CH_3$
16	R = 4-NO_2Ph-	R' = $-CH_2-(CH_2)_4-CH_3$
17	R = Ph-	R' = $-CH_2-(CH_2)_{10}-CH_3$
18	R = 4-NO_2Ph-	R' = $-CH_2-(CH_2)_{10}-CH_3$
19	R = $PhCH_2O$ -	R' = 4-NO_2Ph-

Scheme 2.

Results and Discussion

A library of molecules containing different aliphatic (C_{12}, C_6, or C_3 alkyl radicals) and aromatic (phenyl and 4-nitrophenyl) end chains were prepared. Most of the synthesized compounds bear different end groups on the peptide termini and a few of them are "symmetrically" substituted, bearing analogous side chains on both ends of the peptide (compounds **4**, **5**, and **6**). The synthesis of these molecules was carried out by using conventional peptide chemistry methods (Scheme 2). A convergent approach was used and tetrapeptide derivatives **4**–**18** were obtained by coupling the corresponding dipeptide derivatives with the use of EDC or DCC as coupling reagents. The preparation of *N*-acylated dipeptides **3** was carried out by a Schotten–Baumann procedure. Compounds **2a**–**c** were prepared by amide formation on the C-terminus of the Z-protected dipeptides and subsequent removal of the protecting group. All these compounds were fully characterized by NMR spectroscopy and mass spectrometry (see Experimental Section).

Gelation Studies

Firstly, the gelation capability of the compounds with alkyl end groups (**4**–**13**) in organic solvents was studied, and the results are collected in Table 1. In general, all compounds were poorly soluble and had to be heated at the boiling temperature of the solvent to obtain a clear solution. After cooling to room temperature many of them formed gels and some gave place to phase separation by formation of aggregates that could not be defined as proper gels but as weak gels or colloidal precipitates. In general, gels were obtained both in polar and apolar solvents, and most of them were transparent at their minimum gel concentration (mgc).

It is interesting to compare the gelation properties of the compounds that present analogous alkyl chains on both ends of the peptide (compounds **4**, **5**, and **6**, which present respectively C_{12}, C_6, and C_3 chains). It can be observed that in the more polar solvents the compound with C_6 chains (**5**) is in general a better gelator than **4** (C_{12} chains), which does not form proper gels in alcohols. It could be argued that in compound **4** the long C_{12} end chains preclude gel formation in polar solvents. Although solvophobic interactions are expected to be important for aliphatic chains in polar solvents, it seems that the long and flexible C_{12} chains may not be contributing significantly to the 1D aggregation motif shown in Scheme 1.

Table 1. Gelation behavior of compounds **4**–**12** (5 mg/mL).[a]

Solvent	Compound								
	4	**5**	**6**	**7**	**8**	**9**	**10**	**11**	**12**
Methanol	A	WG	WG	P	G (10)	G (9)	WG	A	G (12)
Ethanol	WG	G (11)	G (13)	G	G (10)	G (9)	G (12)	G (10)	G (12)
2-Propanol	A	G (7)	WG	G (9)	G (3)	G (7)	G (5)	A	G (12)
Cyclohexanol	S	G (11)	G (13)	A/P	G (10)	G (9)	G (12)	G (10)	G (12)
Acetone	WG	G (11)	G (13)	WG	I/A	A	I	A	P
THF	G (8)	G (11)	A	G (9)	I/A	G (9)	I	Pc	Pc
DME	A	G (7)	I	WG	WG	A	P	A	Pc
CH_3CN	G (8)	G (4)	WG	WG	G (6)	G (7)	G (7)	A	G (12)
CH_2Cl_2	G (8)	G (11)	I	G (9)	WG	G (9)	G (12)	Pc	Pc
$CHCl_3$	G (8)	G (11)	I	G (9)	WG	G (9)	G (12)	WG	Pc
Dioxane	WG	G (11)	A	G (9)	WG	WG	G (12)	Pc	Pc
Cyclohexane	WG	A/Pc	A	A/P	A	G (9)	P	Pc	Pc
Toluene	G (8)	G (9)	Pc	WG	G (8)	G (6)	G (10)	WG	Pc

[a] G = gel, WG = weak gel, P = precipitate, Pc = colloidal, I = insoluble, A = aggregates, S = soluble. Minimum gel concentration (mM) in parentheses.

On the other hand, if the gelation capabilities of compounds **5** (C_6 end chains) and **6** (C_3 end chains) are compared it can be noticed that significant differences are observed in solvents that present low or moderate polarity. For example, in toluene compound **5** forms gels at a mgc value of 9 mM, whereas compound **6** forms a precipitate. This behavior is related to that observed, for instance, in dichloromethane where compound **5** forms a gel, whereas compound **6** is insoluble. These results can be easily rationalized by realizing that hydrogen-bonding interactions can be dominant in solvents of low-to-moderate polarity and that in these solvents the alkyl chains may play a role in the solubilization of the molecules by favorable interactions with the solvent. In the case of molecule **6**, the reported behaviors could be ascribed to the fact that the C_3 chains are too short. They would preclude the formation the long aggregates required for fiber formation as a result of the insoluble nature of the associated species. On the contrary, C_6 (and C_{12}) chains would impart the required solubility, for example, in toluene. This line of reasoning would explain the fact that in the most apolar solvent, cyclohexane, gels are formed only with the compound with C_{12} chains, **4**.

If the gelation capabilities of the compounds that present different alkyl chains on both ends are considered (compounds **6**–**12**) it can be observed again that in apolar solvents the presence of short C_3 chains is not favorable for gel formation. For example, compounds **6**, **11**, and **12** are not capable of gel formation in toluene. The only compound in the series that contains C_3 end chains and forms gels in solvents of low polarity is **8**, which presents a C_{12} chain that would compensate for the presence of the C_3 chain on the other end. The data in Table 1 in general suggest that the compounds with similar alkyl chains on both ends are better gelators. For example, in acetone proper gels are only formed by compounds **5** (C_6 chains on both ends) and **6** (C_3 chains) and weak gels are formed by compounds **4** (C_{12} chains) and **7** (C_{12}, C_6 chains). All the other compounds, which present dissimilar alkyl chains on both ends, do not form gels in acetone. These results suggest that in compounds with similar end chains the interactions among the apolar moieties are strengthened relative to the case of unsymmetrical compounds favoring the formation of gels.

In order to assess in more detail the role played by the aliphatic end groups in gelation, the replacement of one of the alkyl tails by an aromatic fragment was studied. In general, the substitution of alkyl moieties by aromatic moieties had a significant effect on the gelation behavior. For example, compound **5** (C_6, C_6) forms gels in toluene, but replacement of one C_6 moiety by a phenyl or 4-nitrophenyl group (compounds **15** and **16**, respectively) gives place to insoluble materials in this solvent. A similar tendency can be observed for compound **4** (C_{12}, C_{12}), which is a good gelator in toluene, but it is transformed into a weak gelator in the case of compound **17** and into insoluble species in the case of **18**. Clearly, these results indicate that in apolar solvents the aliphatic moieties play a relevant role in the formation of fibrillar structures that cannot be paralleled with the use of aromatic moieties. Most likely, the aliphatic moieties provide this family of molecules with more intense intermolecular interactions and a better packing capability relative to those of analogous molecules with aromatic end groups. Indeed, compounds bearing two aromatic end groups (i.e. compound **19**) failed to form gels.

It is interesting to note that in a solvent of intermediate polarity, such as THF, compound **6** (C_3, C_3) is not a gelator but its aromatic analogue with one phenyl end group (**13**) is capable of forming gels. This fact could be the result of improved solvation of the phenyl moieties as compared to the C_3 units, which would avoid precipitation of the aggregates. Finally, the more polar 4-nitrophenyl analogue (compound **14**) does not form gels in the range of solvents studied.

Spectroscopic Studies

FTIR spectroscopy is a useful technique to investigate the secondary structure of peptides and proteins.[14] For all the studied dialkyl compounds (**4**–**12**), the amide I band

appeared at 1625 cm^{-1}, which is typical for the strong H-bonding of the β-sheet secondary structure. Moreover, a weak band appeared at 1695 cm^{-1} indicating a high content of antiparallel β-sheet organization, in agreement with our previous results on compound **4** (see for instance Figure 1 for compound **5** and Supporting Information). It is noteworthy that the FTIR spectra of dried gels of compounds with aromatic end units such as compounds **15** and **17** showed the presence of a broad absorption band in the amide I region, with several overlapping peaks revealing not only an antiparallel β-sheet organization (1698 cm^{-1}) but also other randomly organized assemblies (1682, 1668, 1650 cm^{-1}, see Supporting Information). This indicates that replacement of one of the alkyl units by a phenyl moiety generates weaker intermolecular interactions between aromatic and alkyl groups in the antiparallel arrangement relative to those found in the compounds with two alkyl groups. In this way, the clear preference for the antiparallel arrangement found in compounds **4**–**12** is lost in analogues **13**–**18** with aromatic units, which would present also other aggregation modes including a parallel β-sheet disposition among them (Figure 2).

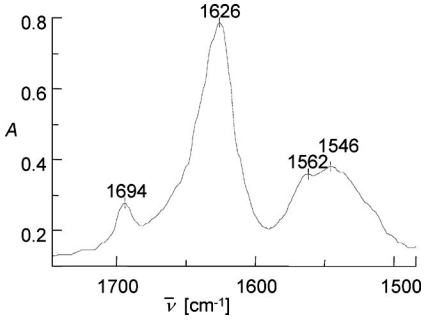

Figure 1. FTIR of the amide C=O region of xerogel of compound **5**.

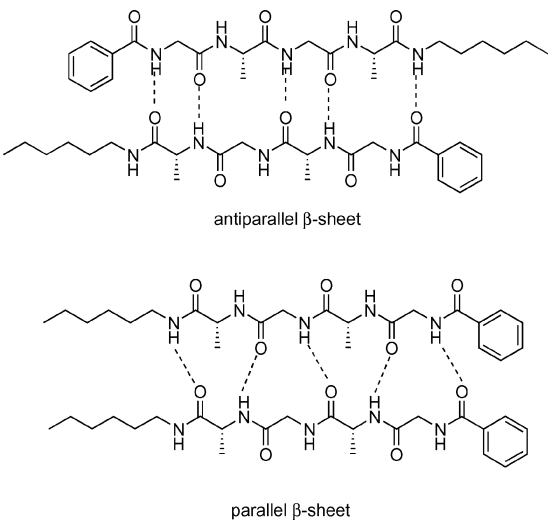

Figure 2. Proposed antiparallel and parallel arrangements for compound **15**.

Circular dichroism was also used to support the formation of β-sheet type-aggregates.[15] Solid-state spectra of xerogels were recorded and, in all the cases, a pattern typical for this arrangement was observed: a negative band with a maximum at ca. 220 nm, and crossing zero at ca. 210 nm, and in some cases a positive lobe at 195 nm (see for instance Figure 3 for compound **5** and Supporting Information).

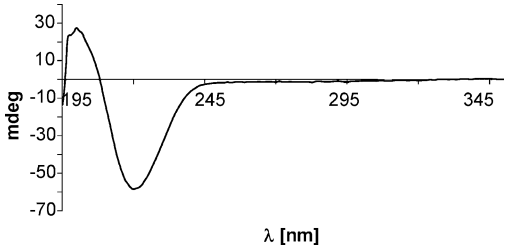

Figure 3. CD spectrum of a xerogel of compound **5** (from a toluene gel).

X-ray Powder Diffraction

Wide-angle X-ray diffraction (WAXD) spectra of the xerogels were in good agreement with the proposed β-sheet arrangement. In all the cases, a low-angle sharp peak corresponding approximately to a calculated distance for a fully extended molecule was obtained. For example, for compound **5**, the WAXD data of xerogels obtained from different solvents provided in all the cases peaks corresponding to a periodicity of 30 Å, which fits nicely with the calculated distance for an extended molecule. Additionally, in all the cases, peaks assigned to a periodic distance of 4.4 Å were found, which can be ascribed to extended two-dimensional layers of β-sheets that stack parallel on top of each other (see Figure 4 and Supporting Information for other compounds).

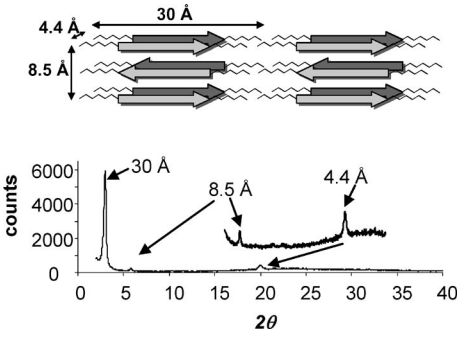

Figure 4. Proposed packing model (top) and WAXD pattern (bottom) for xerogels of compound **5**.

For a given compound, there were not important differences in the position of the diffraction peaks between different solvents. This fact reveals that although macroscopic properties such as solubility or gelation efficiency are strongly solvent dependent, the solvent has a limited effect in the organization at the molecular level. Only some subtle

differences were observed for the related low-angle peaks, probably, with a different degree of mobility of the tails. Higher angle peaks, corresponding to shorter distances in the microcrystalline structure, were sometimes absent, especially in xerogels from apolar solvents, which also showed broader bands than in polar ones. This is probably due to a higher extent of tail mobility that could provoke the presence of some folded segments within the chain.

In natural silk fibers, the antiparallel organization is achieved through an intramolecular turn of the polypeptidic chain, and the repeating distance corresponds to the H-bonding direction of ca. 9.4 Å.[16] In our case, where this turn is not present, we found two different situations: (i) compounds bearing C_{12} tails, which showed a spacing of ca. 11 Å and (ii) compounds with shorter length tails, which presented shorter spacing (8.5 Å). In the first case, the greater chain mobility of the longest tails could explain the observed larger spacing, whereas in the second, shorter tails resulted in more compact packing.

At a higher level of organization, two different packing models may be proposed for the arrangement of the antiparallel β-sheets, namely, head-to-head or head-to-tail (see Scheme 3). For symmetrically substituted compounds, only the head-to-tail packing fits with the observed low-angle diffraction peaks, coincident with the fully extended molecular dimension. A head-to-head packing would produce larger repeating distances than those obtained experimentally. Similarly, in the case of unsymmetrically substituted compounds, head-to-tail packing also fits with the experimental data and a head-to-head packing seems less likely because it would cause kinks and folds in the chains with the result of a loss of packing efficiency.

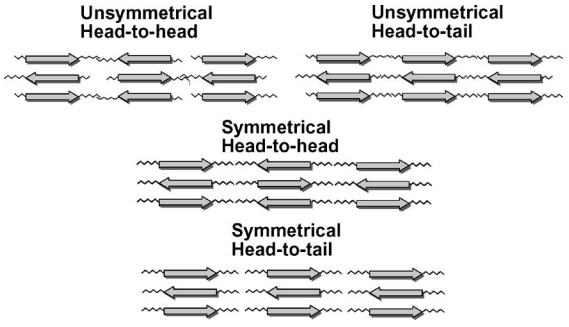

Scheme 3.

Electron Microscopy Studies

The microscopic aspect of the gels and fibrillar aggregates obtained was studied by scanning electron microscopy. For this purpose, aggregates were dried and the xerogels were investigated. These compounds presented a high tendency to form fibrillar architectures. Fibers and fibrils were observed in most of the cases with differences in length, stiffness, and branching degree, revealing that these compounds have a great tendency to form elongated objects (Figures 5, 6, and 7). Some of them further entangled to form networks whereas others merged into rigid and long ribbons, or even fused into globular objects with membrane-like aspect.

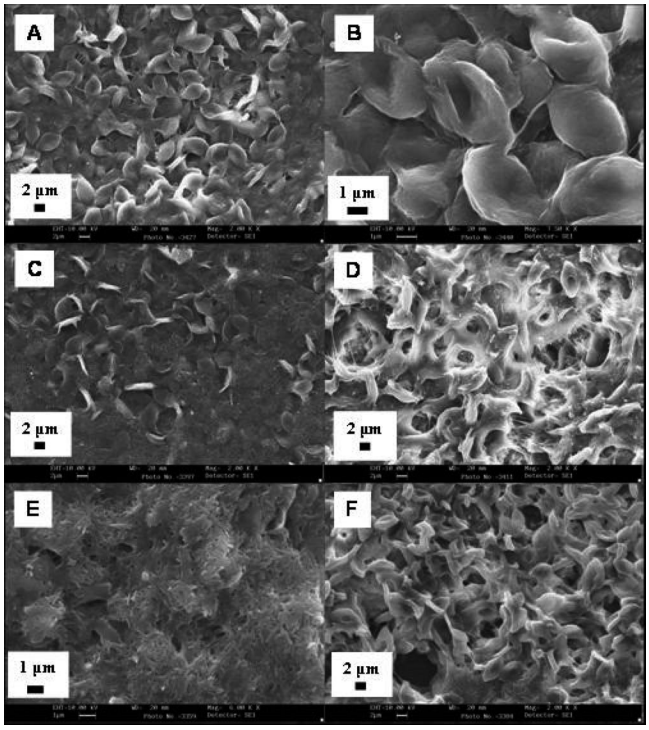

Figure 5. SEM images of xerogels and colloidal precipitates from compounds **5** (A,B), **6** (C), **8** (D), **10** (E), and **12** (F) gels in toluene.

Although WAXD studies have revealed that all the studied molecules are present with basically the same organization at the molecular level, the gel network showed a diversity of morphologies depending mainly on the solvent. For instance, the network of xerogels obtained from toluene is formed by tiny fibrils of less than 100 nm width that are fused forming bags of micrometer size that were probably filled by solvent in the original gels (Figure 5).[13] Even for compounds **6** and **12**, which did not form strong gels, a similar morphology was observed with only subtle differences at the microscopic level. In difference, xerogels from acetonitrile (Figure 6) revealed a network made by very long and thin fibers, with several hundreds of nanometers in width and tens of micrometers in length, that in some cases appeared highly aligned (**5** and **10**), whereas in other cases showed a higher tendency for coiling and cross linking (**7**, **8**, **9**, and **12**). For xerogels prepared from alcohols (Figure 7), very long and thin fibers were also observed in general. However in the case of compound **11** a different aspect was observed in methanol. In this case, fibers were significantly shorter, and in consequence, the formation of a network was not complete and isolated aggregates were formed instead of a strong gel. The xerogel from compound **8** was also different, but in this case, a higher degree of cross-linking could be observed, in agreement with the formation of a strong gel in that solvent.

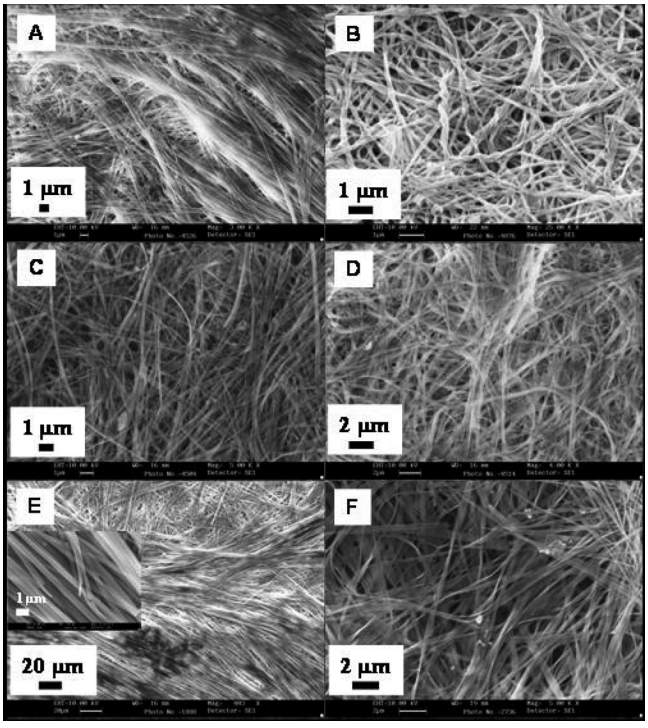

Figure 6. SEM images of xerogels from compounds **5** (A), **7** (B), **8** (C), **9** (D), **10** (E), and **12** (F) gels in acetonitrile.

From this behavior, it may be concluded that, for those compounds that formed gels, the nature of the side chains does not seem to affect significantly the microscopic aspect of the xerogel for a given solvent being the formation of fibrillar networks a general trend. Only in the cases where a strong gel was not formed, namely aggregates or precipitates being formed instead, were different morphologies observed.

Taking into account all the structural information discussed above and the fact that all these compounds, despite the fact that they show different specific morphologies, assemble into fibrillar aggregates, we may propose a model for their hierarchical organization into microscopic size fibers. In a first level of organization, molecular entities assemble to form an antiparallel β-sheet secondary structure, with a vague influence of the length of the alkyl chains. These extended sheets stack into parallel layers separated by 4.4 Å in all the cases. These layers have a preferential one-dimensional growth that produces fibers directed by the formation of H-bonds parallel to their axes. This arrangement is known as the cross-β structure and is typical for amyloid-like fibrils and some silk fibroins (Figure 8).[8,17]

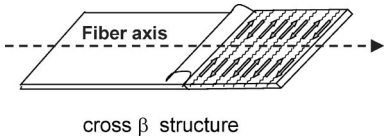

Figure 8. Proposed cross-β packing.

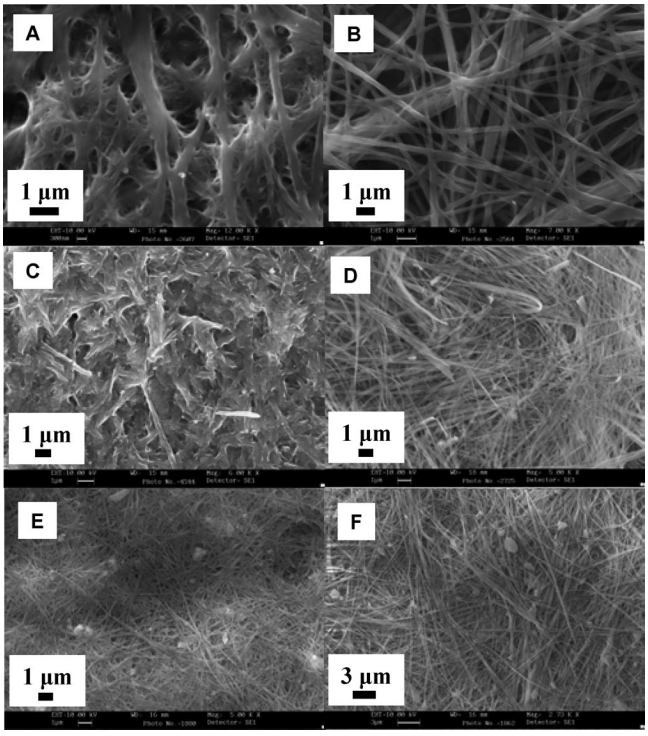

Figure 7. SEM images of xerogels from compounds **8** (A), **10** (B), **11** (C), and **12** (D) gels in methanol and **5** (E) and **8** (F) in 2-propanol.

The potential influence of side groups in the self-assembly of oligopeptides and its effect on the fiber packing has been reported. In our case, as in other reported, it seems reasonable that the strongest interaction, H-bonding, runs parallel to the fiber axis and that interactions between tails have a smaller contribution to the resulting elongated objects.[18] This model would explain why fibrillar aggregates are always found for those compounds that formed gels, independently of the chain length. Thus, the effectiveness of the interaction between tails would affect the thickness of the fibers, and to some extent the length of the fiber. For instance, packing of symmetrical tails would lead to a more stable situation than for unsymmetrical ones, where intercalation or folding may produce packing mistakes and kinks.

Conclusions

We have studied in detail the aggregation behavior of a series of silk-inspired low molecular weight compounds containing a β-sheet-like H-bonding core and apolar end groups. It has been shown that these molecules present a high tendency to form fibrillar networks, which in many cases produced gels. The results have provided useful information on the role played by the apolar alkyl chains in the

self-assembly. It has been noticed that the length of the apolar moiety can affect directly the gelation capabilities of these molecules and this behavior can be associated to factors such as solubility and intermolecular interactions. The presence of similar alkyl chains on both ends of the molecule has been shown to improve the gelation properties, most likely due to favorable packing of the β-sheet like stacks. Structural studies of the aggregation at the molecular level with FTIR, circular dichroism, and WAXD revealed that all the alkyl-terminated gelators present an antiparallel β-sheet-type arrangement. However, replacement of the alkyl end groups by aromatic end groups results in the formation of materials where different structural motifs coexist (antiparallel and parallel β-sheet for example). Having in mind that strong H-bonding interactions are possible both in the parallel and antiparallel arrangements, these results indicate that alkyl groups play a key role in the observed antiparallel structures. This fact can be ascribed to factors such as packing efficiency, solvophobic effects, and favorable van der Waals interactions. Finally, a variety of microscopic morphologies associated with really small changes in molecular structure and solvent have been observed in the SEM study of the xerogels.

Overall, the results reveal that this is a family of versatile gelators, because the fine tuning of their structure permits the formation of gels in a broad range of solvents of different polarity. Identically, the microscopic aspect of the material can also be regulated by simple structural changes and this property is interesting in fields associated to nanofabrication. Most interestingly, the fidelity found for the antiparallel β-sheet motif opens the door for the use of this tetrapeptidic structure as a scaffold for the construction of highly ordered functional materials with application, for example, in materials science and catalysis.

Experimental Section

General Procedure for Compounds 1a–c: Benzyloxycarbonylglycyl–L-alanine (3.57 mmol) was dissolved in freshly dried DME (80 mL) in a round-bottomed flask with a stirrer and immersed in an ice bath. Dicyclohexylcarbodiimide (DCC; 4.6 mmol) dissolved in DME (100 mL) was then added dropwise to the solution over a period of 1 h, and the mixture was stirred for 2 h. Then, the amine (3.5 mmol) dissolved in dry DME was added slowly, and the mixture was warmed to room temperature overnight. Afterwards, the white suspension was filtered, and the solvent was evaporated under vacuum. The product was purified by column chromatography on (silica gel; CH_2Cl_2/MeOH).

***N*-Propyl-(*N*′-benzyloxycarbonylglycyl)-L-alanine Amide (1a):** White solid (1.55 g, 62% yield). M.p. 117–120 °C. R_f = 0.59 (CH_2Cl_2/MeOH, 96:4). ^{1}H NMR (300 MHz, [D$_6$]DMSO, 30 °C): δ = 0.78 (t, J = 7.2 Hz, 3 H), 1.16 (d, J = 6.9 Hz, 3 H), 1.30 (m, 2 H), 2.93 (q, J = 6.6 Hz, 2 H), 3.61 (d, J = 5.7 Hz, 2 H), 4.19 (m, 1 H), 5.01 (s, 2 H), 7.35 (s, 5 H), 7.41 (t, J = 5.4 Hz, 1 H), 7.80 (s, 1 H), 7.94 (d, J = 7.2 Hz, 1 H) ppm. ^{13}C NMR (75 MHz, [D$_6$]DMSO, 30 °C): δ = 11.97, 19.23, 22.92, 44.21, 48.85, 66.14, 128.32, 128.46, 129.03, 137.73, 157.21, 169.30, 172.55 ppm. IR: $\tilde{\nu}$ = 3307, 3268, 2961, 2850, 1723, 1691, 1646, 1542, 1267 cm^{-1}. HRMS (ESI-TOF+): calcd. for $C_{16}H_{23}N_3O_4Na^+$ [M + Na]$^+$ 344.1581; found 344.1587 (Δ = 1.7 ppm), 665.21 [2M + Na]$^+$.

***N*-Hexyl-(*N*′-benzyloxycarbonylglycyl)-L-alanine Amide (1b):** White solid (2.34 g, 78% yield). M.p. 115–117 °C. R_f = 0.63 (CH_2Cl_2/MeOH, 96:4). ^{1}H NMR (300 MHz, [D$_6$]DMSO, 30 °C): δ = 0.81 (t, J = 6.3 Hz, 3 H), 1.16 (m, 9 H), 1.34 (t, J = 6.3 Hz, 2 H), 2.97 (q, J = 6.3 Hz, 2 H), 3.61 (d, J = 5.7 Hz, 2 H), 4.21 (m, 1 H), 5.01 (s, 2 H), 7.35 (s, 5 H), 7.43 (t, J = 5.7 Hz, 1 H), 7.77 (s, 1 H), 7.93 (d, J = 7.5 Hz, 1 H) ppm. ^{13}C NMR (75 MHz, [D$_6$]DMSO, 30 °C): δ = 14.55, 19.20, 22.68, 26.61, 29.60, 31.60, 39.18, 44.21, 48.83, 66.13, 128.31, 128.46, 129.02, 137.72, 157.21, 169.29, 172.47 ppm. IR: $\tilde{\nu}$ = 3314, 3079, 2930, 2857, 1736, 1674, 1653, 1536, 1256 cm^{-1}. HRMS (ESI-TOF+): calcd. for $C_{19}H_{29}N_3O_4Na^+$ [M + Na]$^+$ 386.2056; found 386.2049 (Δ = 1.8 ppm), 749.32 [2M + Na]$^+$, 364.22 [M + H]$^+$.

***N*-Dodecyl-(*N*′-benzyloxycarbonylglycyl)-L-alanine Amide (1c):** White solid (2.3 g, 92% yield). M.p. 121–124 °C. R_f = 0.68 (CH_2Cl_2/MeOH, 90:10). ^{1}H NMR (300 MHz, [D$_6$]DMSO, 30 °C): δ = 0.81 (t, J = 6.3 Hz, 3 H), 1.15–1.25 (m, 21 H), 1.34 (t, J = 5.7 Hz, 2 H), 2.97 (q, J = 6.3 Hz, 2 H), 3.60 (d, J = 6 Hz, 2 H), 4.19 (m, 1 H), 5.01 (s, 2 H), 7.33 (s, 5 H), 7.44 (t, J = 6.0 Hz, 1 H), 7.76 (s, 1 H), 7.77 (d, J = 7.5 Hz, 1 H) ppm. ^{13}C NMR (75 MHz, [D$_6$]DMSO, 30 °C): δ = 14.62, 19.27, 22.76, 26.97, 2C (29.37), 5C (29.66), 31.96, 39.18, 44.23, 48.81, 66.13, 128.31, 128.44, 129.01, 137.72, 157.19, 169.25, 172.42 ppm. IR: $\tilde{\nu}$ = 3321, 3070, 2921, 2850, 1726, 1687, 1653, 1546, 1272 cm^{-1}. HRMS (ESI-TOF+): calcd. for $C_{25}H_{41}N_3O_4Na^+$ [M + Na]$^+$ 470.2995; found 470.3002 (Δ = 1.4 ppm), 917.4327 [2M + Na]$^+$, 448.3202 [M + Na]$^+$.

General Procedure for Compounds 2a–c: Compound **1** (1.43 mmol) was dissolved in methanol (30 mL) containing palladium on activated carbon (5 wt.-%, 50 mg) in a two-necked, round-bottomed flask. Then a balloon filled with hydrogen gas was connected to one neck of the flask and the system was saturated with hydrogen by slightly opening and closing the second neck to remove air. After complete deprotection, the solution was filtered through Celite, and the filtrate was evaporated under vacuum. The product was purified through a silica column (CH_2Cl_2/MeOH).

***N*-Propyl-(*N*′-glycyl)-L-alanine Amide (2a):** White solid (1.51 g, 98% yield). M.p. 290 °C (decomp.). R_f = 0.37 (MeOH/CH_2Cl_2, 25:75). ^{1}H NMR (300 MHz, [D$_6$]DMSO, 30 °C): δ = 0.83 (t, J = 7.2 Hz, 3 H), 1.17 (d, J = 7.5 Hz, 3 H), 1.35–1.41 (m, 2 H), 2.99 (m, 2 H), 3.10 (s, 2 H) 4.55 (m, 1 H), 7.90 (s, 1 H), 8.02 (d, 1 H) ppm. ^{13}C NMR (75 MHz, [D$_6$]DMSO, 30 °C): δ = 11.96, 19.70, 22.93, 39.36, 44.93, 48.46, 172.46, 172.63 ppm. IR: $\tilde{\nu}$ = 3292, 2967, 2850, 1646, 1545, 1458, 1254 cm^{-1}. HRMS (ESI-TOF+): calcd. for $C_8H_{17}N_3O_2Na^+$ [M + Na]$^+$ 210.1213; found 210.1176 (Δ = 19.0 ppm), 397.2142 [2M + Na]$^+$.

***N*-Hexyl-(*N*′-glycyl)-L-alanine Amide (2b):** White solid (2.2 g, 97% yield). M.p. 82–84 °C. R_f = 0.42 (MeOH/CH_2Cl_2, 25:75). ^{1}H NMR (300 MHz, [D$_6$]DMSO, 30 °C): δ = 0.82 (t, J = 6.6 Hz, 3 H), 1.16 (m, 11 H), 1.34 (t, J = 6.6 Hz, 2 H), 3.00 (m, 2 H), 3.03 (m, 2 H), 4.24 (m, 1 H), 7.88 (t, J = 5.1 Hz, 1 H), 8.02 (s, 1 H) ppm. ^{13}C NMR (75 MHz, [D$_6$]DMSO, 30 °C): δ = 14.77, 19.95, 22.92, 26.84, 29.85, 31.82, 39.35, 45.29, 48.62, 172.75, 172.83 ppm. IR: $\tilde{\nu}$ = 3283, 2930, 2853, 1647, 1511, 1458, 1251 cm^{-1}. HRMS (ESI-TOF): calcd. for $C_{11}H_{23}N_3O_2Na^+$ [M + Na]$^+$ 252.1682; found 252.1639 (Δ = 17.0 ppm), 481.2881 [2M + Na]$^+$.

***N*-Dodecyl-(*N*′-glycyl)-L-alanine Amide (2c):** White solid (2.2 g, 98% yield). M.p. 88–89 °C. R_f = 0.51 (MeOH/CH_2Cl_2, 25:75). ^{1}H NMR (300 MHz, [D$_6$]DMSO, 30 °C): δ = 0.81 (t, J = 6.3 Hz, 3 H), 1.17–1.23 (m, 23 H), 1.34 (t, J = 6.6 Hz, 2 H), 2.97 (m, 2 H), 3.11

(s, 2 H), 4.26 (m, 1 H), 7.91 (t, J = 5.7 Hz, 1 H), 8.28 (d, J = 6.9 Hz, 1 H) ppm. ^{13}C NMR (75 MHz, [D$_6$]DMSO, 30 °C): δ = 14.62, 19.48, 22.75, 26.96, 2C (29.37), 5C (29.65), 31.95, 39.15, 42.62, 48.81, 168.88, 172.28 ppm. IR: $\tilde{\nu}$ = 3298, 2930, 2849, 1647, 1561, 1459, 1248 cm^{-1}. HRMS (ESI-TOF+): calcd. for $C_{17}H_{35}N_3O_2Na^+$ [M + Na]$^+$ 336.2621; found 336.2663 (Δ = 10.0 ppm).

General Procedure for Compounds 3a–c: Glycyl-L-alanine (6.8 mmol) dissolved in NaOH (1 M, 50 mL) was placed in a round-bottomed flask with an efficient magnetic stirrer. The flask was completely immersed in an ice bath and during the reaction the stirrer was set in very rapid motion. To the solution was dropwise added pure acyl chloride (13.6 mmol) and NaOH (1 M, 10 mL) at the same rate in such a way that the pH of the reaction mixture did not decrease below 10. When the reaction was complete, the suspension was acidified carefully with 2 M HCl. The residue obtained after filtration was extracted with petroleum ether to remove the fatty acid. The final dipeptide derivative was chromatographed on a silica gel column (MeOH/CH_2Cl_2).

Propanoylglycyl-L-alanine (3a): White solid (0.8 g, 82% yield). M.p. 104–107 °C. R_f = 0.25 (MeOH/CH_2Cl_2, 10:90). ^{1}H NMR (300 MHz, [D$_6$]DMSO, 30 °C): δ = 0.94 (t, J = 7.5 Hz, 3 H), 1.22–1.25 (m, 3 H), 2.07 (q, J = 7.8 Hz, 2 H), 3.66 (m, 2 H), 4.22 (m, 1 H), 7.96 (d, J = 5.4 Hz, 1 H), 8.07 (d, J = 7.2 Hz, 1 H), 12.55 (br. s, 1 H) ppm. ^{13}C NMR (75 MHz, [D$_6$]DMSO, 30 °C): δ = 10.29, 17.80, 17.83, 28.80, 42.15, 47.93, 47.99, 169.30, 173.72, 174.49 ppm. IR: $\tilde{\nu}$ = 3386, 3273, 3098, 2984, 2531, 1743, 1633, 1577, 1210 cm^{-1}. HRMS (ESI-TOF+): calcd. for $C_8H_{14}N_2O_4Na^+$ [M + Na]$^+$ 225.0846; found 225.0861 (Δ = 6.6 ppm).

Hexanoylglycyl-L-alanine (3b): White solid (0.98 g, 89% yield). M.p. 125–127 °C. ^{1}H NMR (300 MHz, [D$_6$]DMSO, 30 °C): δ = 0.81 (t, J = 6.6 Hz, 3 H), 1.21–1.25 (m, 7 H), 1.45 (q, J = 7.2 Hz, 2 H), 2.07 (t, J = 7.5 Hz, 2 H), 3.66 (m, 2 H), 4.16 (m, 1 H), 7.95 (t, J = 5.4 Hz, 1 H), 8.05 (d, J = 7.5 Hz, 1 H), 12.54 (br. s, 1 H) ppm. ^{13}C NMR (75 MHz, [D$_6$]DMSO, 30 °C): δ = 14.52, 18.00, 22.55, 25.52, 31.55, 35.82, 42.32, 48.12, 169.44, 173.20, 174.63 ppm. IR: $\tilde{\nu}$ = 3292, 3102, 2859, 2570, 1734, 1641, 1570, 1209 cm^{-1}. HRMS (ESI-TOF+): calcd. for $C_{11}H_{20}N_2O_4Na^+$ [M + Na]$^+$ 267.1315; found 267.1324 (Δ = 3.3 ppm), 511.2747 [2M + Na]$^+$.

Dodecanoylglycyl-L-alanine (3c): White solid (0.94 g, 94% yield). M.p. 133–135 °C. ^{1}H NMR (300 MHz, [D$_6$]DMSO, 30 °C): δ = 0.81 (t, J = 6.0 Hz, 3 H), 1.20–1.25 (m, 19 H), 1.46 (s, 2 H), 2.06 (t, J = 7.2 Hz, 2 H), 3.62 (m, 2 H), 4.19 (m, 1 H), 7.91 (t, J = 5.4 Hz, 1 H), 8.03 (d, J = 7.5 Hz, 1 H), 12.45 (s, 1 H) ppm. ^{13}C NMR (75 MHz, [D$_6$]DMSO, 30 °C): δ = 14.62, 18.00, 22.77, 25.86, 29.35, 29.38, 29.50, 29.61, 29.68, 29.71, 31.98, 35.86, 42.30, 48.08, 169.41, 172.15, 174.64 ppm. IR: $\tilde{\nu}$ = 3289, 3102, 2850, 2570, 1726, 1641, 1570, 1208 cm^{-1}. HRMS (ESI-TOF+): calcd. for $C_{17}H_{32}N_2O_4Na^+$ [M + Na]$^+$ 351.2254; found 351.2254 (Δ = 0.0 ppm), 679.4482 [2M + Na]$^+$.

Benzoylglycyl-L-alanine (3d): White solid (0.91 g, 91% yield). M.p. 187–189 °C. R_f = 0.51 (MeOH/CH_2Cl_2,10:90). ^{1}H NMR (300 MHz, [D$_6$]DMSO, 30 °C): δ = 1.26 (d, J = 7.2 Hz, 3 H), 3.87 (m, 2 H), 4.20 (m, 1 H), 7.43–7.53 (m, 3 H), 7.85 (dd, J = 6.6, 1.8 Hz, 2 H), 8.19 (d, J = 5.1 Hz, 1 H), 8.65 (t, J = 7.5 Hz, 1 H), 12.14 (br. s, 1 H) ppm. ^{13}C NMR (75 MHz, [D$_6$]DMSO, 30 °C): δ = 18.02, 42.94, 48.20, 128.00, 128.96, 132.00, 134.74, 167.13, 169.38, 174.68 ppm. IR: $\tilde{\nu}$ = 3518, 3382, 3075, 2929, 1715, 1626, 1492, 1293 cm^{-1}. HRMS (ESI-TOF+): calcd. for $C_{12}H_{14}N_2O_4Na^+$ [M + Na]$^+$ 273.0846; found 273.08567 (Δ = 3.9 ppm), 523.1891 [2M + Na]$^+$.

(4-Nitrobenzoyl)glycyl-L-alanine (3e): White solid (0.89 g, 89% yield). M.p. 194–198 °C. R_f = 0.54 (MeOH/CH_2Cl_2, 10:90). ^{1}H NMR (300 MHz, [D$_6$]DMSO, 30 °C): δ = 1.25 (d, J = 8.7 Hz, 3 H), 3.92 (m, J = 6 Hz, 2 H), 4.20 (m, 1 H), 8.07 (d, J = 8.7 Hz, 2 H), 8.25 (m, 3 H), 9.03 (t, J = 6 Hz, 1 H), 12.47 (br. s, 1 H) ppm. ^{13}C NMR (75 MHz, [D$_6$]DMSO, 30 °C): δ = 22.73, 47.75, 52.95, 128.94, 134.28, 145.16, 154.53, 170.27, 173.68, 179.38 ppm. IR: $\tilde{\nu}$ = 3518, 3290, 3075, 2929, 1724, 1687, 1656, 1531, 1348 cm^{-1}. HRMS (ESI-TOF+): calcd. for $C_{12}H_{13}N_3O_6Na^+$ [M + Na]$^+$ 318,0697; found 318.0710 (Δ = 4.0 ppm).

General Procedure for Compounds 4–12

Method 1: Compound **3** (0.567 mmol) and HOBT (0.684 mol) were placed in a round-bottomed flask with a stirrer and dissolved in freshly dried DMF (10 mL). The flask was immersed in an ice bath. To the mixture was dropwise added DCC (0.73 mmol) dissolved in dry DMF (5 mL). The mixture was stirred for 2 h and then, amine **2** (0.567 mmol) dissolved in dry DMF was added dropwise. The mixture was further stirred overnight at room temperature. Afterwards, the reaction mixture was quenched by adding an excess amount of diethyl ether and it was then washed with water. The white product was purified through 4–5-cm packed column with silica by (CH_2Cl_2/MeOH, 90:10) firstly and then with pure methanol or ethanol.

Method 2: Compound **3** (0.567 mmol), HOBT (0.684 mmol), EDC (0.627 mmol), and amine **2** (0.567 mmol) were stirred overnight in freshly dried DMF (10 mL). Then, DMF was evaporated under vacuum, and the solid material was ground, washed with an excess amount of water, and dried under high vacuum.

***N*-Dodecyl-(*N′*-dodecanoylglycyl-L-alanylglycyl)-L-alanine Amide (4):** Described previously.[13]

***N*-Hexyl-[*N′*-hexanoylglycyl-L-alanylglycyl]-L-alanine Amide (5):** Method 1: White solid (0.35 g, 89% yield). M.p. 244–248 °C. ^{1}H NMR (300 MHz, [D$_6$]DMSO, 30 °C): δ = 0.81 (t, J = 6.0 Hz, 3 H), 1.15–1.36 (m, 21 H), 1.46 (m, 2 H), 2.06 (t, J = 7.2 Hz, 2 H), 2.99 (m, 2 H), 3.64 (m, 4 H), 4.17 (m, 2 H), 7.73 (m, 1 H), 7.79 (m, 1 H), 8.00 (m, 1 H), 8.09 (m, 1 H), 8.19 (m, 1 H) ppm. ^{13}C NMR (75 MHz, [D$_6$]DMSO, 30 °C): δ = 14.42, 14.48, 14.53, 18.37, 18.88, 22.51, 22.22, 25.48, 26.56, 29.54, 31.51, 31.57, 35.78, 42.65, 42.84, 48.94, 49.31, 169.03, 169.94, 172.55, 173.49, 173.64 ppm. IR: $\tilde{\nu}$ = 3292, 2929, 2859, 1696, 1626, 1545, 1448, 1233 cm^{-1}. HRMS (ESI-TOF+): calcd. for $C_{22}H_{41}N_5NaO_5^+$ [M + Na]$^+$ 478.30; found 478.2986 (Δ = 2.9 ppm).

***N*-Propyl-[*N′*-propanoylglycyl-L-alanylglycyl]-L-alanine Amide (6):** Method 2: White solid (0.14 g, 72% yield). M.p. 274–275 °C. ^{1}H NMR (300 MHz, [D$_6$]DMSO, 30 °C): δ = 0.79 (t, J = 4.5 Hz, 3 H), 0.95 (t, J = 4.5 Hz, 3 H), 1.15–1.21 (m, 6 H), 1.34–1.42 (m, 2 H), 2.09 (q, J = 4.5 Hz, 2 H), 2.96–3.02 (m, 2 H), 3.62 (m, 4 H), 4.22 (m, 2 H), 7.71 (t, J = 3.3 Hz, 1 H), 7.79 (d, J = 4.5 Hz, 1 H), 7.94 (t, J = 3.3 Hz, 1 H), 8.09 (d, J = 4.5 Hz, 1 H), 8.15 (t, J = 3.3 Hz, 1 H) ppm. ^{13}C NMR (75 MHz, [D$_6$]DMSO, 30 °C): δ = 10.64, 12.18, 18.77, 19.21, 23.15, 29.16, 39.61, 42.87, 43.07, 49.13, 49.43, 169.17, 170.06, 172.72, 173.61, 174.29 ppm. IR: $\tilde{\nu}$ = 3291, 3088, 2970, 2876, 1694, 1626, 1543, 1444, 1235 cm^{-1}. HRMS (ESI-TOF+): calcd. for $C_{16}H_{29}N_5NaO_5^+$ [M + Na]$^+$ 394.2061; found 394.2068 (Δ = 1.7 ppm).

***N*-Hexyl-[*N′*-dodecanoylglycyl-L-alanylglycyl]-L-alanine Amide (7):** Method 1: White solid (0.29 g, 89% yield). M.p. 258–263 °C. ^{1}H NMR (300 MHz, [D$_6$]DMSO, 30 °C): δ = 0.81 (t, J = 6.9 Hz, 3 H), 1.19 (s, 31 H), 1.33 (t, J = 6.6 Hz, 2 H), 1.43 (t, J = 6.6 Hz, 2 H), 2.06 (t, J = 6.9 Hz, 2 H), 3.00 (s, 2 H), 3.64 (m, 4 H), 4.15 (m, 2 H), 7.70 (m, 2 H), 7.95 (s, 1 H), 8.06 (m, 2 H) ppm. ^{13}C NMR

(75 MHz, [D$_6$]DMSO, 30 °C): δ = 14.54, 14.60, 18.36, 18.39, 18.47, 18.97, 22.68, 22.74, 25.81, 26.60, 29.35, 29.47, 29.58, 29.65, 29.68, 31.60, 31.94, 35.82, 39.19, 42.65, 42.85, 48.90, 49.23, 168.90, 169.84, 172.42, 173.35, 173.40 ppm. IR: $\tilde{\nu}$ = 3296, 2925, 2854, 1696, 1627, 1560, 1449, 1238 cm^{-1}. HRMS (ESI-TOF+): calcd. for $C_{28}H_{53}N_5NaO_5^+$ [M + Na]$^+$ 562.3939; found 562.3918 (Δ = 3.7 ppm).

***N*-Propyl-[*N'*-docecanoylglycyl-L-alanylglycyl]-L-alanine Amide (8):** Method 1: White solid (0.27 g, 92% yield). M.p. 259–262 °C. ^{1}H NMR (300 MHz, [D$_6$]DMSO, 30 °C): δ = 0.80 (m, 6 H), 1.191–1.24 (m, 20 H), 1.37–1.49 (m, 6 H), 2.09 (t, J = 7.5 Hz, 2 H), 2.97 (s, 2 H) 3.68 (m, J = 4.5 Hz, 4 H), 4.20 (m, 2 H), 7.50 (s, 1 H), 7.58 (s, 1 H), 7.73 (s, 1 H), 7.83 (s, 1 H), 7.95 (s, 1 H) ppm. ^{13}C NMR (75 MHz, [D$_6$]DMSO, 30 °C): δ = 11.97, 14.63, 18.56, 19.01, 22.77, 22.92, 25.84, 29.36, 29.38, 29.49, 29.60, 29.68, 29.70, 31.97, 35.82, 39.38, 42.62, 42.83, 48.90, 49.19, 168.93, 169.81, 172.50, 173.32, 173.34 ppm. HRMS (ESI-TOF+): calcd. for $C_{25}H_{47}N_5NaO_5^+$ [M + Na]$^+$ 520.3469; found 520.3478 (Δ = 1.7 ppm).

***N*-Dodecyl-[*N'*-hexanoylglycyl-L-alanylglycyl]-L-alanine Amide (9):** Method 1: White solid (0.29 g, 86% yield). M.p. 264–267 °C. ^{1}H NMR (300 MHz, [D$_6$]DMSO, 30 °C): δ = 0.82 (t, J = 6.3 Hz, 3 H), 1.15–1.21 (m, 33 H), 1.45 (m, 2 H), 2.09 (t, J = 7.2 Hz, 2 H), 3.01 (m, 2 H), 3.66 (m, 4 H), 4.17 (m, 2 H), 7.60 (s, 1 H), 7.69 (d, J = 6.6 Hz, 1 H), 7.88 (s, 1 H), 8.01 (s, 1 H), 8.14 (s, 1 H) ppm. ^{13}C NMR (75 MHz, [D$_6$]DMSO, 30 °C): δ = 14.39, 14.49, 18.46, 18.94, 22.47, 22.67, 25.11, 25.45, 26.97, 29.29, 29.36, 3C (29.61), 31.57, 31.91, 35.88, 39.21, 39.63, 42.92, 43.08, 49.03, 49.36, 168.95, 169.88, 172.47, 173.35, 173.38 ppm. IR: $\tilde{\nu}$ = 3293, 2925, 2854, 1696, 1622, 1560, 1448, 1235 cm^{-1}. HRMS (ESI-TOF+): calcd. for $C_{28}H_{53}N_5NaO_5^+$ [M + Na]$^+$ 562.3939; found 562.3923 (Δ = 2.8 ppm).

***N*-Propyl-[*N'*-hexanoylglycyl-L-alanylglycyl]-L-alanine Amide (10):** Method 1: White solid (0.26 g, 87% yield). M.p. 244–245 °C. ^{1}H NMR (300 MHz, [D$_6$]DMSO, 30 °C): δ = 0.78 (m, 6 H), 1.16–1.23 (m, 10 H), 1.34–1.51 (m, 4 H), 2.06 (t, J = 7.5 Hz, 2 H), 2.94 (q, J = 6.9 Hz, 2 H), 3.64 (m, 4 H), 4.16 (m, 2 H), 7.72 (t, J = 5.4 Hz, 1 H), 7.81 (d, J = 7.5 Hz, 1 H), 7.97 (t, J = 5.4 Hz, 1 H), 8.09 (d, J = 6.6 Hz, 1 H), 8.18 (t, J = 5.4 Hz, 1 H) ppm. ^{13}C NMR (75 MHz, [D$_6$]DMSO, 30 °C): δ = 11.96, 14.25, 18.58, 19.01, 22.56, 22.92, 25.52, 31.55, 35.78, 42.63, 42.83, 48.90, 49.18, 49.27, 168.94, 169.81, 172.50, 173.34, 173.37 ppm. IR: $\tilde{\nu}$ = 3293, 2961, 2854, 1696, 1622, 1542, 1444, 1248 cm^{-1}. HRMS (ESI-TOF+): calcd. for $C_{19}H_{35}N_5NaO_5^+$ [M + Na]$^+$ 436.253; found 436.2520 (Δ = 2.2 ppm), 413.2654 [M + H]$^+$.

***N*-Dodecyl-[*N'*-propanoylglycyl-L-alanylglycyl]-L-alanine Amide (11):** Method 2: White solid (0.31 g, 98% yield). M.p. 234–238 °C. ^{1}H NMR (300 MHz, [D$_6$]DMSO, 30 °C): δ = 0.81 (t, J = 6.9 Hz, 3 H), 0.85 (t, J = 7.5 Hz, 3 H), 1.15–1.22 (m, 11 H), 1.35 (s, 2 H), 2.07 (q, J = 7.5 Hz, 2 H), 2.99 (s, 2 H), 3.68 (m, 4 H), 4.17 (m, 2 H), 7.74 (s, 1 H), 7.82 (d, J = 6 Hz, 1 H), 7.99 (m, 1 H), 8.15 (m, 2 H) ppm. ^{13}C NMR (75 MHz, [D$_6$]DMSO, 30 °C): δ = 10.45, 14.59, 18.57, 19.04, 19.19, 33.73, 26.64, 28.94, 29.65, 31.64, 32.96, 39.21, 42.67, 42.86, 48.81, 48.91, 49.22, 168.94, 169.86, 172.44, 173.39, 174.08 ppm. IR: $\tilde{\nu}$ = 3290, 3084, 2925, 2854, 1694, 1626, 1545, 1444, 1234 cm^{-1}. HRMS (ESI-TOF+): calcd. for $C_{22}H_{34}N_6NaO_5^+$ [M + Na]$^+$ 520.3469; found 520.3458 (Δ = 1.9 ppm).

***N*-Hexyl-[*N'*-propanoylglycyl-L-alanylglycyl]-L-alanine Amide (12):** Method 2: White solid (0.31 g, 78% yield). M.p. 269–271 °C. ^{1}H NMR (300 MHz, [D$_6$]DMSO, 30 °C): δ = 0.81 (t, J = 6.3 Hz, 3 H), 0.95 (t, J = 6.3 Hz, 3 H), 1.15–1.21 (m, 12 H), 1.35 (q, J = 7.8 Hz, 2 H), 2.06 (q, J = 7.8 Hz, 2 H), 2.98 (d, J = 7.8 Hz, 2 H), 3.66 (m, 4 H), 4.17 (m, 2 H), 7.72 (t, J = 3.3 Hz, 1 H), 7.79 (d, J = 4.0 Hz, 1 H), 7.96 (t, J = 3.3 Hz, 1 H), 8.10 (d, J = 4.0 Hz, 1 H), 8.16 (t, J = 3.6 Hz, 1 H) ppm. ^{13}C NMR (75 MHz, [D$_6$]DMSO, 30 °C): δ = 10.45, 14.59, 18.57, 19.04, 22.73, 26.64, 28.95, 29.65, 31.64, 39.21, 42.67, 42.86, 48.90, 49.22, 168.95, 169.87, 172.45, 173.41, 174.08 ppm. IR: $\tilde{\nu}$ = 3291, 3089, 2930, 2859, 1694, 1626, 1545, 1443, 1235 cm^{-1}. HRMS (ESI-TOF+): calcd. for $C_{19}H_{35}N_5NaO_5^+$ [M + Na]$^+$ 436.2530; found 436.2554 (Δ = 5.5 ppm), 849.5322 [2M + Na]$^+$.

***N*-Propyl-[*N'*-benzoylglycyl-L-alanylglycyl]-L-alanine Amide (13):** Method 1: White powder (0.26 g, 85% yield). M.p. 233.5 °C. R_f = 0.46 (MeOH/CH_2Cl_2, 10:90). ^{1}H NMR (300 MHz, [D$_6$]DMSO, 30 °C): δ = 0.76 (t, J = 7.2 Hz, 3 H), 1.11 (d, J = 7.2 Hz, 3 H), 1.17 (d, J = 7.2 Hz, 3 H), 1.35–1.42 (m, 2 H), 2.93 (t, J = 6.6 Hz, 2 H), 3.67 (m, 2 H), 3.90 (m, 3 H), 4.14–4.27 (m, 2 H), 7.42 (m, 2 H), 7.69 (t, J = 5.1 Hz, 1 H), 7.78 (m, 3 H), 8.21 (t, J = 6.6 Hz, 2 H), 8.69 (t, J = 5.1 Hz, 1 H) ppm. ^{13}C NMR (75 MHz, [D$_6$]DMSO, 30 °C): δ = 11.95, 18.55, 18.94, 22.91, 39.40, 42.87, 43.26, 48.91, 49.32, 127.97, 128.95, 132.02, 134.63, 167.25, 168.95, 169.78, 172.48, 173.40 ppm. IR: $\tilde{\nu}$ = 3283, 2969, 2854, 1696, 1622, 1542, 1446, 1234 cm^{-1}. HRMS (ESI-TOF+): calcd. for $C_{20}H_{29}N_5NaO_5^+$ [M + Na]$^+$ 442.2061; found 442.2061 (Δ = 0.0 ppm).

***N*-Propyl-[*N'*-(4-nitrobenzoyl)glycyl-L-alanylglycyl]-L-alanine Amide (14):** Method 2: White powder (0.19 g, 77% yield). M.p. 249–253 °C. R_f = 0.43 (MeOH/CH_2Cl_2, 10:90). ^{1}H NMR (300 MHz, [D$_6$]DMSO, 30 °C): δ = 0.75 (t, J = 7.2 Hz, 3 H), 1.11 (d, J = 6.9 Hz, 3 H), 1.22 (d, J = 6.9 Hz, 3 H), 1.32 (m, 2 H), 2.93 (d, J = 6.9 Hz, 2 H), 3.63 (m, 2 H), 3.88 (m, 2 H), 4.13 (m, 1 H), 4.22 (m, 1 H), 7.69 (t, J = 5.4 Hz, 1 H), 7.72 (d, J = 7.2 Hz, 1 H), 8.05 (d, J = 8.7 Hz, 2 H), 8.18 (t, J = 5.4 Hz, 1 H), 8.28 (t, J = 8.1 Hz, 3 H), 9.02 (t, J = 5.4 Hz, 1 H) ppm. ^{13}C NMR (75 MHz, [D$_6$]DMSO, 30 °C): δ = 11.90, 18.43, 18.87, 22.86, 39.24, 42.84, 43.26, 48.96, 49.41, 124.20, 129.50, 140.27, 149.80, 165.77, 169.04, 169.42, 172.60, 173.47 ppm. IR: $\tilde{\nu}$ = 3280, 2922, 2854, 1696, 16226, 1545, 1448, 1349 cm^{-1}. HRMS (ESI-TOF+): calcd. for $C_{20}H_{28}N_6NaO_7^+$ [M + Na]$^+$ 487.1912; found 487.1914 (Δ = 0.4 ppm).

***N*-Hexyl-[*N'*-benzoylglycyl-L-alanylglycyl]-L-alanine Amide (15):** Method 1: White powder (0.24 g, 80% yield). M.p. 238 °C. R_f = 0.58 (MeOH/CH_2Cl_2, 10:90). ^{1}H NMR (300 MHz, [D$_6$]DMSO, 30 °C): δ = 0.81 (t, J = 6.9 Hz, 3 H), 1.13 (d, J = 7.2 Hz, 3 H), 1.14–1.35 (m, 11 H), 1.34–1.42 (m, 2 H), 2.98 (d, J = 5.7 Hz, 2 H), 3.66 (m, 2 H), 3.89 (m, 2 H), 4.16–4.25 (m, 2 H), 7.42 (m, 3 H), 7.68 (s, 1 H), 7.76 (d, J = 7.8 Hz, 1 H), 7.83 (d, J = 8.4 Hz, 1 H), 8.18 (t, J = 6.9 Hz, 1 H), 8.69 (t, J = 6.9 Hz, 1 H) ppm. ^{13}C NMR (75 MHz, [D$_6$]DMSO, 30 °C): δ = 14.54, 18.42, 18.84, 22.67, 26.56, 29.55, 31.58, 39.28, 42.88, 43.26, 48.93, 49.42, 127.95, 128.96, 132.06, 134.54, 167.35, 169.01, 169.89, 172.49, 173.48 ppm. IR: $\tilde{\nu}$ = 3283, 2929, 2857, 1696, 1622, 1542, 1448, 1235 cm^{-1}. HRMS (ESI-TOF+): calcd. for $C_{23}H_{35}N_5NaO_5^+$ [M + Na]$^+$ 484.253; found 484.2521 (Δ = 1.8 ppm), 945.3710 [2M + Na]$^+$.

***N*-Hexyl-[*N'*-(4-nitrobenzoyl)glycyl-L-alanylglycyl]-L-alanine Amide (16):** Method 1: White powder (0.25 g, 81% yield). M.p. 258.4 °C. R_f = 0.34 (MeOH/CH_2Cl_2, 10:90). ^{1}H NMR (300 MHz, [D$_6$]-DMSO, 30 °C): δ = 0.86 (t, J = 6.6 Hz, 3 H), 1.11 (d, J = 7.2 Hz, 3 H), 1.22 (m, 9 H), 1.34 (t, J = 6.3 Hz, 2 H), 2.97 (m, 2 H), 3.68 (t, J = 6.3 Hz, 2 H), 3.94 (d, J = 6.3 Hz, 2 H), 4.14–4.28 (m, 2 H), 7.69 (t, J = 6.6 Hz, 1 H), 7.78 (d, J = 7.5 Hz, 1 H), 8.07 (d, J = 9.0 Hz, 2 H), 8.19 (t, J = 6.3 Hz, 1 H), 8.27 (m, 3 H), 9.03 (t, J = 5.1 Hz, 1 H) ppm. ^{13}C NMR (75 MHz, [D$_6$]DMSO, 30 °C): δ = 14.36, 18.49, 18.54, 22.66, 26.56, 29.55, 31.57, 39.67, 43.21, 43.23, 48.82, 49.28, 124.04, 129.37, 140.26, 149.76, 165.62, 168.90, 169.29,

172.41, 173.33 ppm. IR: ṽ = 3300, 2930, 2854, 1696, 1629, 1528, 1443, 1238 cm^{-1}. HRMS (ESI-TOF+): calcd. for $C_{23}H_{34}N_6NaO_7^+$ [M + Na]$^+$ 529.2381; found 529.2352 (Δ = 5.4 ppm).

***N*-Dodecyl-[*N*′-benzoylglycyl-L-alanylglycyl]-L-alanine Amide (17):** Method 1: White powder (0.17 g, 80% yield). M.p. 277.2 °C. R_f = 0.58 (MeOH/CH_2Cl_2, 10:90). ^{1}H NMR (300 MHz, [D$_6$]DMSO, 30 °C): δ = 080 (t, *J* = 6.6 Hz, 3 H), 1.10 (d, *J* = 7.2 Hz, 3 H), 1.20–1.33 (m, 23 H), 2.97 (m, 2 H), 3.65 (m, 2 H), 3.88 (m, 2 H), 4.10–4.25 (m, 2 H), 7.44–7.51 (m, 3 H), 7.68 (t, *J* = 5 Hz, 1 H), 7.77 (d, *J* = 6 Hz, 1 H), 7.83 (dd, *J* = 6.9, 1.5 Hz, 2 H), 8.19 (m, 2 H), 8.70 (t, *J* = 5 Hz, 1 H) ppm. ^{13}C NMR (75 MHz, [D$_6$]DMSO, 30 °C): δ = 14.60, 18.45, 18.88, 22.74, 26.92, 3C (29.35), 5C (29.64), 29.69, 31.95, 39.19, 42.87, 43.26, 48.91, 49.37, 127.95, 128.96, 132.05, 134.57, 167.33, 168.97, 169.84, 172.45, 173.44 ppm. IR: ṽ = 3282, 2924, 2853, 1696, 1622, 1542, 1448, 1236 cm^{-1}. HRMS (ESI-TOF+): calcd. for $C_{29}H_{47}N_5NaO_5^+$ [M + Na]$^+$ 568.3469; found 568.3451 (Δ = 3.1 ppm).

***N*-Dodecyl-[*N*′-(4-nitrobenzoyl)glycyl-L-alanylglycyl]-L-alanine Amide (18):** Method 1: White powder (0.27 g, 89% yield). M.p. 247.1 °C. R_f = 0.57 (MeOH/CH_2Cl_2, 10:90). ^{1}H NMR (300 MHz, [D$_6$]-DMSO, 30 °C): δ = 0.83 (t, *J* = 6.3 Hz, 3 H), 1.11–1.24 (m, 26 H), 2.98 (m, 2 H), 3.66 (m, 2 H), 3.93 (m, 2 H), 4.11–4.23 (m, 2 H), 7.71 (t, *J* = 5 Hz, 1 H), 7.81 (d, *J* = 6 Hz, 1 H), 8.08 (m, 3 H), 8.08 (m, 3 H), 9.03 (t, *J* = 5.1 Hz, 1 H) ppm. ^{13}C NMR (75 MHz, [D$_6$] DMSO, 30 °C): δ = 14.52, 16.77, 18.40, 18.85, 22.65, 26.82, 3C (29.26), 5C (29.55), 31.85, 39.14, 42.67, 43.11, 48.75, 49.20, 124.09, 129.39, 140.15, 149.64, 165.50, 168.82, 169.21, 172.31, 173.24 ppm. IR: ṽ = 3299, 2921, 2851, 1696, 1639, 1560, 1451, 1234, 1109 cm^{-1}. HRMS (ESI-TOF+): calcd. for $C_{29}H_{46}N_6NaO_7^+$ [M + Na]$^+$ 613.3320; found 613.3358 (Δ = 6.1 ppm).

Gelation Tests: A given amount of the studied compound was weighted in a screw-capped vial of 20-mm diameter, suspended in 1 mL of solvent and sonicated for 10 min. Then, the vial was heated until the solid was dissolved and afterwards left to spontaneously cool to room temperature. A gel (G) was considered being formed when no gravitational flux was observed upon vial inversion. The term weak gel (WG) was applied to the case where partial fluxion was observed.

Scanning Electron Microscopy: Scanning electron micrographs were taken with a LEO 440I microscope equipped with a digital camera. Samples of the xerogels were prepared by placing the gel on top of a tin plate and, after vacuum drying of the solvent, sputtering with Au/Pd in a Polaron SC7610 Sputter Coater from Fisons Instruments.

Solid State CD: A sample of the gel was dried under vacuum and then KBr discs were prepared by mixing the xerogel (1–2 mg) and dry KBr (200 mg) in an agate mortar and pressing the mixture at 10 ton for ca. 10 min. Transparent discs of less than 0.5 mm were obtained and their CD spectra were randomly taken in at least six different positions of the disc and averaged.[19] Spectra were recorded with a JASCO J-810 spectropolarimeter.

FTIR: KBr pellets of the xerogels were prepared as stated above. Spectra were collected with a JASCO-FTIR-6200 spectrometer.

X-ray Powder Diffraction: Data collection was performed at room temperature with a Bruker D4 Endeavor X-ray powder diffractometer by using Cu-K_α radiation. Samples of the powdered xerogels were placed on a sample holder and data were collected for 2θ values between 2 and 40° with a step size of 0.03° and a time step of 10 s.

Supporting Information (see footnote on the first page of this article): CD, FTIR, powder diffraction, and NMR spectroscopic data for all the described compounds.

Acknowledgments

The authors thank the Spanish Ministry of Science and Innovation (Grant CTQ2006-14984) and Universitat Jaume I (Grant P1 1A2006–01) for funding. S. I. thanks Universitat Jaume I – Bancaixa for a fellowship. Technical assistance by SCIC is also acknowledged.

[1] a) H.-A. Klok, *Angew. Chem. Int. Ed.* **2002**, *41*, 1509–1513; b) J. M. C. van Hest, D. A. Tirrell, *Chem. Commun.* **2001**, 1897–1904; c) J. S. Nowick, *Org. Biomol. Chem.* **2006**, *4*, 3869–3885; d) M. A. B. Block, S. Hecht, *Angew. Chem. Int. Ed.* **2005**, *44*, 6986–6989.

[2] A. Aggeli, N. Boden, S. Zhang (Eds.), *Self-Assembling Peptide Systems in Biology, Medicine and Engineering*, Kluwer, Dordrecht, **2001**.

[3] S. M. Hecht (Ed.), *Bioorganic Chemistry, Peptides and Proteins*, Oxford University Press, New York, **1998**.

[4] a) C. M. Dobson, *Phil. Trans. R. Soc. London B* **2001**, *356*, 133–145; b) O. Sumner Markin, L. C. Serpell, *FEBS J.* **2005**, *272*, 5950–5961; c) R. Krishnan, S. L. Lindquist, *Nature* **2005**, *435*, 765–772.

[5] a) J. Ghanta, C.-L. Shen, L. L. Kiessling, R. M. Murphy, *J. Biol. Chem.* **1996**, *271*, 29525–29528; b) R. C. Elgersma, T. Meijneke, G. Posthuma, D. T. S. Rijkers, R. M. J. Liskamp, *Chem. Eur. J.* **2006**, *12*, 3714–3725; c) J. Sato, T. Takahashi, H. Oshima, S. Matsumura, H. Mihara, *Chem. Eur. J.* **2007**, *13*, 7745–7752; d) R. Mimna, M.-S. Camus, A. Schmid, G. Tuchscherer, H. A. Lashuel, M. Mutter, *Angew. Chem. Int. Ed.* **2007**, *46*, 2681–2684.

[6] a) H. A. Lashuel, S. R. LaBrenz, L. Woo, L. C. Serpell, J. W. Kelly, *J. Am. Chem. Soc.* **2000**, *122*, 5262–5277; b) A. Aggeli, I. A. Nyrkova, M. Bell, R. Harding, L. Carrick, T. C. B. McLeish, A. N. Semenov, N. Boden, *Proc. Natl. Acad. Sci. USA* **2001**, *98*, 11857–11862; c) M. López de la Paz, K. Goldie, J. Zurdo, E. Lacroix, C. M. Dobson, A. Hoenger, L. Serrano, *Proc. Natl. Acad. Sci. USA* **2002**, *99*, 16052–16057; d) H. A. Behanna, J. J. J. M. Donners, A. C. Gordon, S. I. Stupp, *J. Am. Chem. Soc.* **2005**, *127*, 1193–1200; e) S. Deechongkit, E. T. Powers, S.-L. You, J. W. Kelly, *J. Am. Chem. Soc.* **2005**, *127*, 8562–8570.

[7] a) S. K. Maji, D. Haldar, M. G. B. Drew, A. Banerjee, A. K. Das, A. Banerjee, *Tetrahedron* **2004**, *60*, 3251–3259; b) A. Banerjee, A. K. Das, M. G. B. Drew, A. Banerjee, *Tetrahedron* **2005**, *61*, 5906–5914; c) E. Gazit, *FEBS J.* **2005**, *272*, 5971–5978.

[8] I. W. Hamley, *Angew. Chem. Int. Ed.* **2007**, *46*, 8128–8147.

[9] R. G. Weiss, P. Terech (Eds.), *Molecular Gels: Materials with Self-Assembled Fibrillar Networks*, Kluwer, Norwell, **2005**.

[10] F. Fages (Ed.), *Topics in Current Chemistry Vol. 256: Low Molecular Mass Gelators: Design, Self-Assembly, Function*, Springer, New York, **2005**.

[11] a) P. Terech, R. G. Weiss, *Chem. Rev.* **1997**, *97*, 3133–3159; b) D. J. Abdallah, R. G. Weiss, *Adv. Mater.* **2000**, *12*, 1237–1247; c) J. van Esch, B. L. Feringa, *Angew. Chem. Int. Ed.* **2000**, *39*, 2263–2354; d) O. Gronwald, E. Snip, S. Shinkai, *Curr. Opin. Colloid Interface Sci.* **2002**, *7*, 148–156; e) L. A. Estroff, A. D. Hamilton, *Chem. Rev.* **2004**, *104*, 1201–1207; f) A. R. Hirst, D. K. Smith, *Chem. Eur. J.* **2005**, *11*, 5496–5508.

[12] a) B. Escuder, S. Martí, J. F. Miravet, *Langmuir* **2005**, *21*, 6776–6787; b) J. F. Miravet, B. Escuder, *Chem. Commun.* **2005**, 5796–5798.

[13] B. Escuder, J. F. Miravet, *Langmuir* **2006**, *22*, 7793–7797.

[14] P. I. Haris, D. Chapman, *Biopol. Pept. Sci.* **1995**, *37*, 251–263.

[15] N. Sreerama, R. Woody, "Circular Dichroism of Peptides and Proteins" in *Circular Dichroism: Principles and Applications* (Eds.: N. Berova, K. Nakanishi, R. W. Woody), Wiley, New York, **2000**.
[16] Sangappa, S. S. Mahesh, R. J. Somashekar, *Biosci.* **2005**, *30*, 259–268.
[17] a) M. J. Pandya, G. M. Spooner, M. Sunde, J. R. Thorpe, A. Rodger, D. N. Woolfson, *Biochemistry* **2000**, *39*, 8728–8734; b) S. Ramachandran, J. Trewhella, Y. Tseng, Y. B. Yu, *Chem. Mater.* **2006**, *18*, 6157–6162.
[18] T. J. Deming, *Phys. Rev. E: Stat., Nonlinear, Soft Matter Phys.* **2005**, *1*, 28–35.
[19] M. Minguet, D. B. Amabilino, K. Wurst, J. Veciana, *J. Chem. Soc. Perkin Trans. 2* **2001**, 670–676.

Received: June 5, 2008
Published Online: July 29, 2008

